Supplemental material

Valverde et al., https://doi.org/10.1083/jcb.201811139

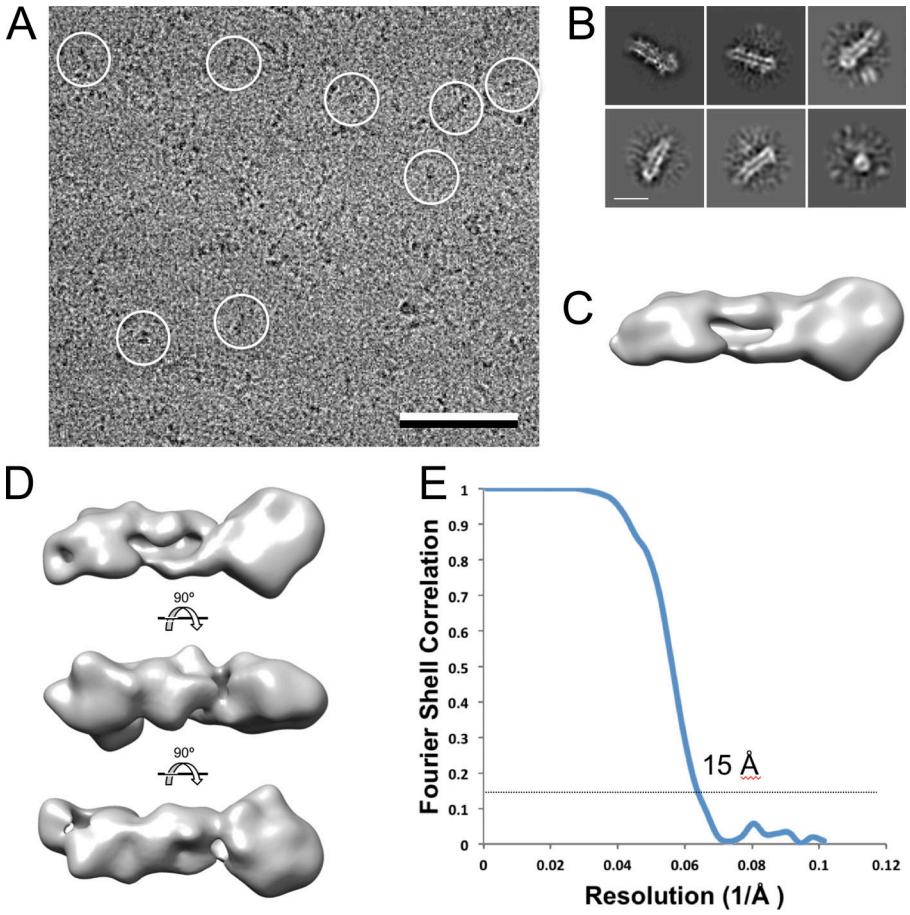

Figure S1. **Cryo-EM reconstruction of human ATG2A. (A)** Area of a motion-corrected cryo-EM image of vitrified ATG2. Some particles are circled. Scale bar: 100 nm. **(B)** Selected 2D class averages. Scale bar: 10 nm. **(C)** Initial model generated in Relion. **(D)** Final density map obtained by refining the entire dataset of 248,086 particles in Relion 2.0. **(E)** Gold-standard FSC curve, indicating a resolution of 15 Å according to the FSC = 0.143 criterion.

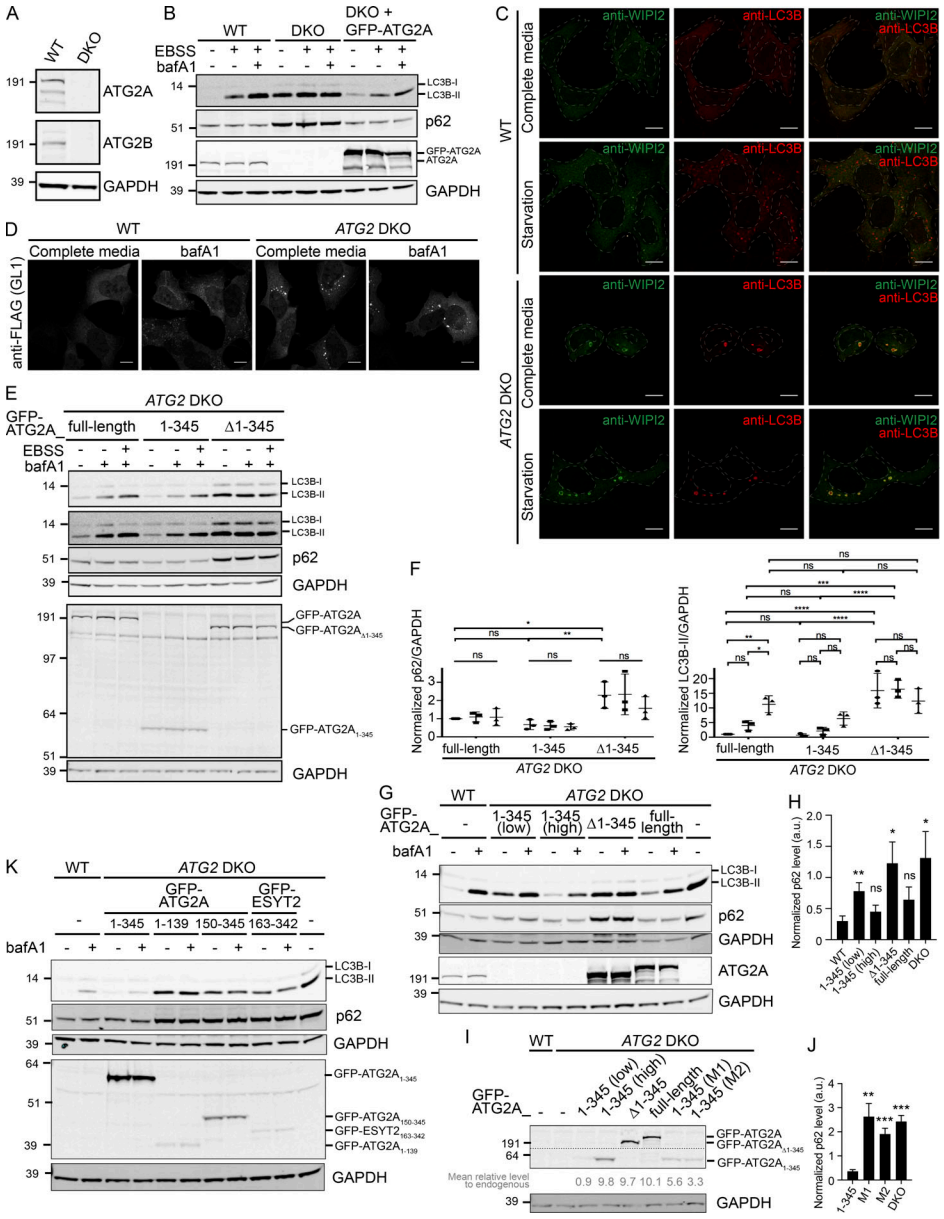

Figure S2. **Rescue of autophagy phenotypes by GFP-ATG2A$_{1–345}$. (A)** Immunoblots of HEK293 *ATG2A/ATG2B* DKO clone 2B7 used throughout this article. **(B)** Immunoblots of WT, DKO, and DKO stably expressing GFP-ATG2A. Note that the GFP-ATG2A rescue restores both bafA1 and starvation + bafA1 flux of LC3B, as well as normal lowered levels of p62. GFP-ATG2A is expressed off the relatively weak PGK promoter, but the levels of GFP-ATG2A are still nearly 10× times higher than endogenous ATG2A in WT cells (shown in I). **(C)** WT cells exhibit a starvation-dependent induction of small WIPI2 and LC3B puncta, while *ATG2* DKO cells constitutively exhibit very large structures that are LC3B- and WIPI2-positive (Velikkakath et al., 2012). Anti-WIPI2 and anti-LC3B immunofluorescent confocal images in WT and DKO cells. Scale bars: 10 µm. **(D)** Very large constitutive GL1 puncta also accumulate in DKO cells. Anti-FLAG IF confocal images in WT and DKO cells stably expressing 3xFLAG-GL1. Scale bars: 10 µm. **(E)** Immunoblots of cellular lysates from *ATG2* DKO HEK293 cells stably expressing one ATG2A construct reveal that GFP-ATG2A$_{1–345}$ is necessary and largely sufficient to rescue LC3B-II and p62 levels. Cells were incubated in complete medium, complete medium plus bafA1, or starvation medium (Earle's balanced salt solution) + bafA1. **(F)** Relative p62 and LC3B-II levels are each normalized to the unstarved and no-bafA1 condition for full-length rescue (first lane in E) and plotted from three independent experiments ± SD. ns, not significant. **(G)** Immunoblots of lysates from WT or DKO cells stably expressing the indicated construct driven by high (CMV) or low (PGK) expression level promoters. Low expression of GFP-ATG2A$_{1–345}$ results in an intermediate autophagy phenotype with incomplete rescue of LC3B-II and p62 levels. **(H)** Relative p62 levels in complete medium (as shown in G) are normalized to the GAPDH loading control and plotted from three independent experiments ± SD. ns, not significant. **(I)** Immunoblots of all stable cell rescues showing relative expression levels of each GFP-tagged protein. Expression relative to endogenous was determined by first comparing expression of full-length GFP-ATG2A to endogenous (as in Fig. S2 G), and then normalizing all GFP-tagged proteins to GFP-ATG2A. Expression levels relative to endogenous are indicated in light gray. **(J)** Relative p62 levels in complete medium for samples from Fig. 3 B are normalized to the GAPDH loading controls and plotted from three independent experiments ± SD. **(K)** Immunoblots of lysates from WT or DKO cells stably expressing indicated constructs. GFP-ATG2A$_{1–139}$ encodes the entirety of the predicted Chorein-N domain (aa 13–131). E-SYT2$_{163–342}$ encodes the lipid transport domain from Extended-Synaptotagmin2. Only GFP-ATG2A$_{1–345}$ restores WT-like low levels of LC3B-II and p62, but note that other constructs do not express as efficiently or are not as stable. Statistical significance was calculated by two-way ANOVA or unpaired *t* tests. *, P < 0.05; **, P < 0.01; ***, P < 0.001; ****, P < 0.0001.

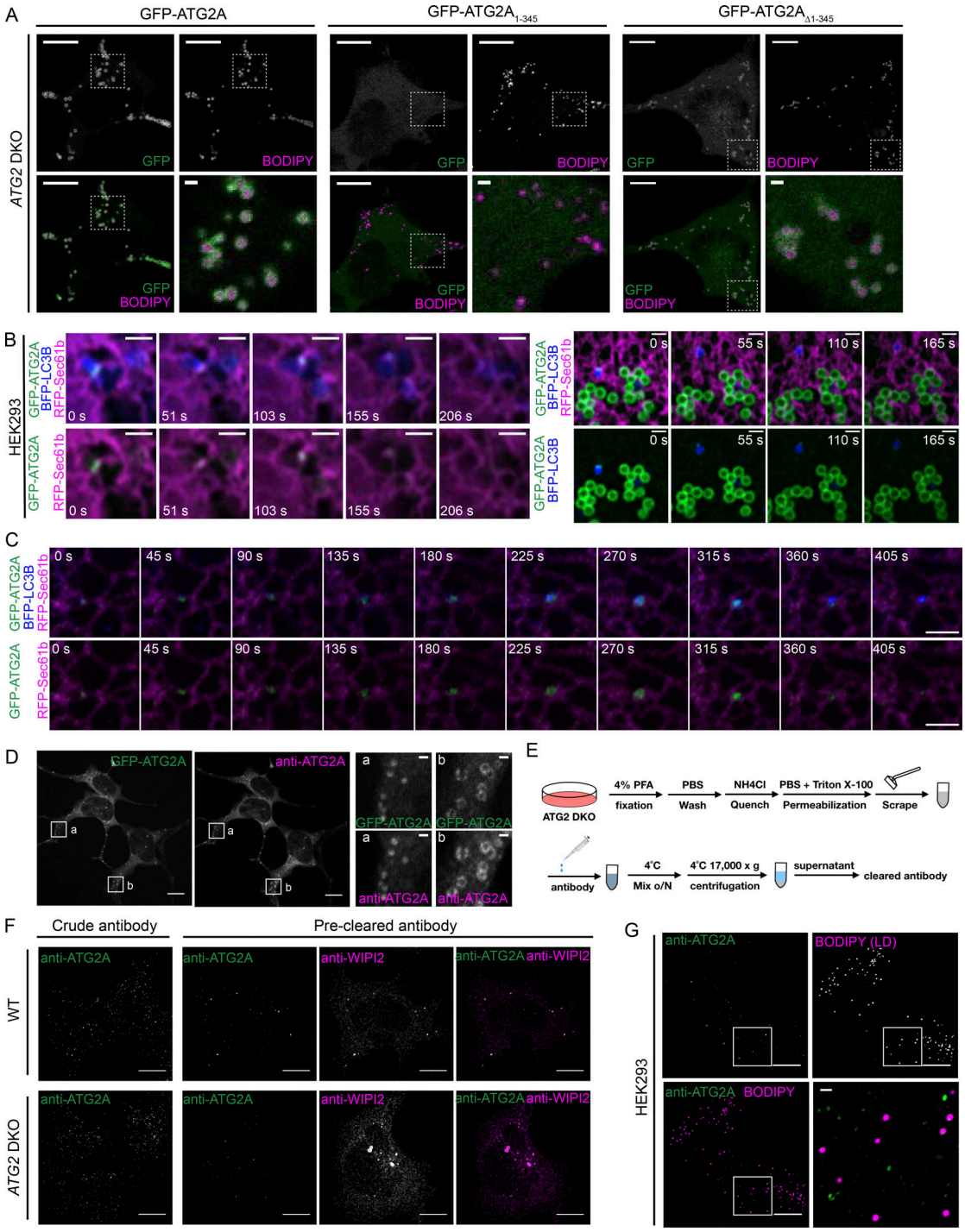

Figure S3. **Localization of GFP-ATG2A and endogenous ATG2A to autophagosomes. (A)** Live imaging of DKO cells incubated with OA and stably expressing indicated GFP-ATG2A protein. LDs are labeled with BODIPY 558/568. Scale bars: 10 µm; zoomed field: 1 µm. **(B)** Still images from two time-lapse recordings of starved *ATG2* DKO cells stably expressing GFP-ATG2A and transiently expressing RFP-Sec61b and BFP-LC3B including the example from Fig. 3 C (left set). Scale bars: 1 µm. **(C)** Still images of time-lapse recording of starved Cos-7 cells stably expressing GFP-ATG2A and transiently expressing RFP-Sec61b and BFP-LC3B. GFP-ATG2A remains associated with the ER throughout 5+ min before disappearing altogether. Scale bars: 1 µm. **(D)** Test of commercial antibody in IF: confocal images of fixed *ATG2* DKO cells stably expressing GFP-ATG2A and anti-ATG2A IF show that ATG2A antibody detects GFP-ATG2A in cells indicating some specificity; however, the background staining is intense, and detection of small puncta consistent with autophagosomes is challenging. **(E)** Cartoon depiction of strategy to clear the anti-ATG2A antibodies of nonspecific binding. *ATG2* DKO cells were fixed, washed, and permeabilized and then collected by scraping. Anti-ATG2A antibody was incubated with this cellular material, and the cellular material was then removed by centrifugation. o/N, overnight. **(F)** Confocal IF images of fixed HEK293 cells after 2 h of starvation stained with either the original commercial antibody (Crude) or the precleared ATG2A antibody and anti-WIPI2. The precleared antibody indicates that the majority of endogenous ATG2A staining is colocalized with WIPI2 structures and is specific (note lack of signal in *ATG2* DKO cells even with gross accumulations of WIPI2). **(G)** Confocal images of fixed HEK293 cells labeled with BODIPY 558/568 and anti-ATG2A IF with cleared antibodies show only occasional adjacent positioning of ATG2A and LDs and no colocalization. Scale bars: 10 µm; zoomed field: 1 µm.

Reference

Velikkakath, A.K., T. Nishimura, E. Oita, N. Ishihara, and N. Mizushima. 2012. Mammalian Atg2 proteins are essential for autophagosome formation and important for regulation of size and distribution of lipid droplets. *Mol. Biol. Cell.* 23:896–909. https://doi.org/10.1091/mbc.e11-09-0785